# Study of the electrochemical synthesis of a hybrid material of Polypyrrole

**Author**
Juan Diego Mantilla Rueda

**Supervisor**
María Teresa Cortés, Ph.D

A thesis submitted in partial fulfillment of the requirements for the degree of Chemist

**Universidad de los Andes**
**Faculty of Sciences**
**Chemistry Department**
**November 2014**

## TABLE OF ABBREVIATIONS

Conductive polymers / Conducting polymers (CPs)

Polypyrrole (PPy)

Polyaniline (PANI)

Politiophene (Pth)

Poliacetylene (PA)

Poli-*p*-phenylene (PPP)

Pyrrole (Py)

4-Amino-1-naphthalenesulfonate ($ANS^-$)

Cyclic voltammetry (CV)

Electrochemical impedance spectroscopy (EIS)

Frequency response analyzer (FRA)

Working electrode (WE)

Counter electrode (CE)

Reference electrode (RE)

Charge transfer resistance ($R_{CT}$)

Solution resistance ($R_{SOL}$)

Double layer capacitance ($C_{DL}$)

Warburg impedance ($Z_W$)

## TABLE OF CONTENTS

# 1. INTRODUCTION

It is usual to think of polymers as common plastics that are used in many fields of everyday life, and in this regard as insulating materials. However, *conductive polymers (CPs),* which are the subject of this study, are quite different from these *normal* polymers due to the fact of being electrical conductors. It must be stressed that CPs are intrinsically conducting and owe their properties to a process of oxidation (or reduction) and *ionic insertion (doping)* instead of conducting fillings such as a metal or carbon particles[1]. Therefore CPs combine the electrical properties of metals with the advantages of polymers and, thus, become greatly useful in the development of many kind of applications such as: supercapacitors[2], solar cells[3], coatings for corrosion protection[4] and electrochemical sensors[5], among others.

The preparation of CPs can be achieved by either chemical or electrochemical methods. The former is preferred when large quantities of material are desired since it is easily scalable whereas the latter is specially useful when CPs for micro-technology are needed[6] and, in general, is more versatile in terms of possible variations and control of polymerization conditions[7]. Both methods have different variables that need to be optimized depending on the characteristics which are desired in the final material.

On the other hand the election of the initial monomer also reflects on the characteristics of the final material. From the innumerable existing options, pyrrole(Py) is one of most extensively used monomers since its polymer (*i.e.* polypyrrole,PPy) posses very useful properties, such as : redox activity, ion exchange and ion discrimination capacities, catalytic activity and corrosion protection properties, among others[7].

Therefore this study presents the optimization of the synthesis of a hybrid material of PPy doped with 4-Amino-1-naphthalenesulfonate ($ANS^-$) on a glassy carbon electrode (GCE). It will be demonstrated that the pulse potentiostatic method is the most adequate for producing a PPy/$ANS^-$ film. Furthermore, PPy/$ANS^-$ is shown to have cationic exchange properties that are used to incorporate Cu(II). This final material (PPy/$ANS^-$/Cu(II)) was shown to improve the current responses in *in-vitro* Dopamine(DA) detection with respect to PPy/$ANS^-$ thus providing initial ground in the development of a non-enzymatic DA selective sensor.

# 2. THEORY

## 2.1. Conductive polymers (CPs)

Polymers have been commonly related with plastics and, consequently, with materials whose properties are opposed to those of metals due to being insulating[8]. However, this changed with Alan J. Heeger, Alan G. MacDiarmid and Hideki Shirakawa who, around 1977, discovered that poly(acetylene) (PA) could reach conductivities of the order of $10^3$ $Sm^{-1}$ when "doped" (oxidized) with iodine, chlorine or bromine vapors. The conductivity reached by this material was higher than that of any known polymer at the time and, thus PA would become the first *conductive polymer* (CP). The Nobel Prize in Chemistry 2000 would be awarded to Heeger, McDiarmird and Shirakawa "*for the discovery and development of conductive polymers"* [8].

Even though PA showed exceptional conductivities, it was unstable in presence of oxygen and moisture and, thus, was never widely used. Therefore different CPs have been developed from new monomers (Figure 1). In general, CPs have in common the fact that they are conjugated and have electronic properties (conductive, magnetic and optics) close to metals and the mechanic properties of conventional polymers[9]. Consequently they have been used in the development of different applications in science and technology which go from materials for energy storage, electrocatalysis, biosensors and artificial muscles, among other things[9].

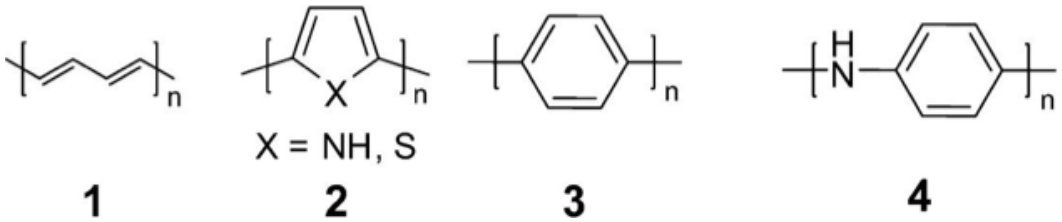


**Figure 1.** Different CPs: 1. polyacetylene(PA); 2.polypyrrole (PPy), Polythiophene (PTh);3. Poli-p-phenylene (PPP); 4. Polyaniline (PANI)[10]

## 2.2. Synthesis of CPs

CPs can be prepared by electrochemical and/or chemical methods. Each of these methods, with an emphasis on the preparation of PPy, is described below.

### 2.2.1. Electrochemical synthesis

It involves the application of an oxidative potential (oxidative polymerization) to a solution of Py and a supporting electrolyte[11]. This potential causes the deposition of the polymer on the anode (Working electrode) surface[6]. The general mechanism of polymerization is shown in Figure 2 and is described in three main steps, as follows: **1)** Oxidation of the monomer to form its corresponding radical cation. This is the rate-determining step. **2)** Coupling between two radicals at the α position due to this is the position with the highest unpaired electron density[12] and the one that leads to a higher degree of conjugation . The repulsion between radicals is assumed to be diminished by the presence of other species such as the solvent, the counter-ion and even the monomer [6]. **3)** Loss of protons to form the aromatic dimer (stabilization step)[12]. The whole process is repeated until the polymeric chain grows enough to exceed the solubility limit and precipitates on the anode surface.

It must be stressed that the electropolymerizaton does not give the neutral non-conducting polypyrrole but rather its oxidized conducting (doped) form. In fact, the final polymeric chain carries a positive charge every 3 to 4 units. This charge is balanced by the incorporation of counter–ions within the planes of oxidized PPy during the oxidation processes and, hence, a hybrid material (conducting polymer-dopant ions) is obtained.

*Step 1*: Oxidation of the monomer Resonant forms

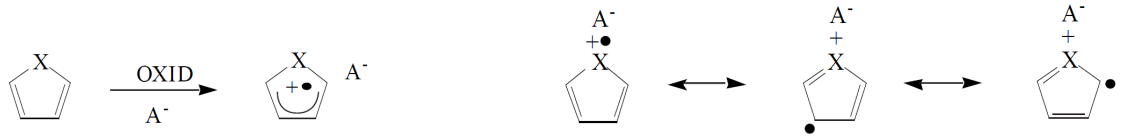


*Step 2*: Radical-radical coupling

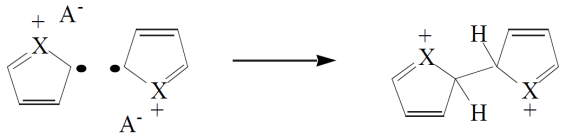


*Step 3*: Loss of protons / Stabilization step

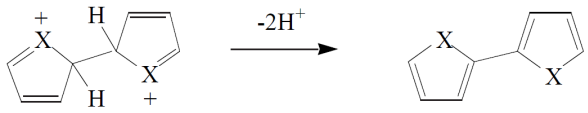


*Step 4*: Chain propagation

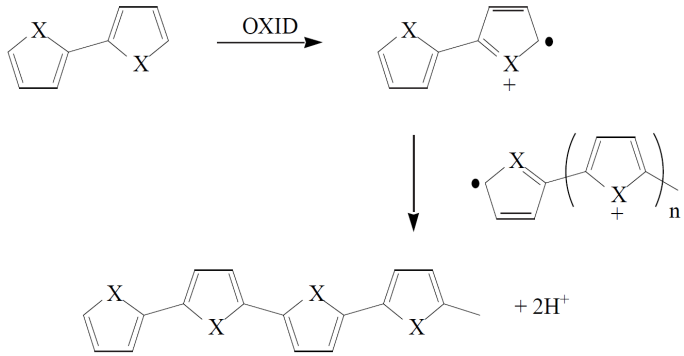


**Figure 2.** Oxidative polymerization mechanism[6]
PPy , X =NH

It is very important to analyze all the synthesis variables since these affect the nature of the process[6] and the properties of the final material. The effects of 6 of these variables are discussed below: **1)** The use of very low potentials causes the rate of polymerization to be so low that the oxidation occurs without precipitation whereas the use of very high potentials (*i.e.* higher than 0.8V vs. Ag/AgCl in the case of PPy) may diminish the polymer conductivity since it is irreversibly oxidized[13]. **2)** Nucleophile solvents or dissolved oxygen may cause secondary reactions with the radical intermediates involved in the process[6]. **3)** The monomer and dopant concentration, as well as its relation are highly decisive in the polymer properties. In particular, if the monomer concentration is too low it can limit the chain growth in the last steps of polymerization. Likewise, the degree of final doping and, in general, the polymerization yield greatly depend on the [dopant]/[monomer] relation. **4)** Additionally, an electrode whose surface is very polar at the synthesis potential may affect the polymer deposition. The influence of the surface is especially clear in the first steps of the polymerization when the nucleation phenomenon must be able to extend all over and produce macromolecules. [6] **5)** On the other hand, the temperature plays and important role in the synthesis efficiency because the former is implied in the transport of reagents and products from and to the reaction zone[6]. **6)** Last, the polymerization method has a significant effect on the morphology of the final polymer[13].

In conclusion, the electrochemical synthesis of CPs is a complex process affected by the competitive nature of the variables involved in the electrodeposition. This makes the study of the electropolymerization of a CP to be a permanent challenge in which the modification of only one parameter may be able to generate a significantly different material.

2.2.1.1. Design of the electrochemical cell

Even though the experimental setup required to induce an electropolymerization is simple, some aspects must be considered. The most common setup uses a three-electrode cell (Figure 3) that consists of a working electrode (W), a reference electrode (R) and a counter electrode (C).The potentiosat applies the desired potential between the W and the R. The reaction of interest takes place on the surface of the W[14] and, thus, the material from which the latter is made becomes an important synthesis variable to take into account. The C provides the current required to sustain the reaction at the W. Therefore, this arrangement prevents large currents from passing through the R and, thus, allows a better potential control[14].

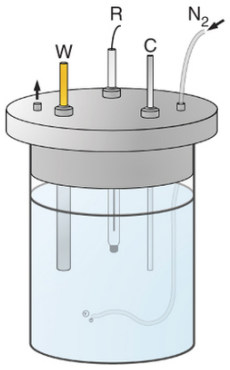


**Figure 3.** Scheme of a 3 electrode electropolymerization cell [15]
W: Working electrode (anode)
R: Reference electrode
C: Counter electrode (cathode)

2.2.1.2. Electrochemical polymerization techniques

There are different methods of electrochemical polymerization within which one can find potentiostatic (constant potential), galvanostatic (constant current) and potendiodynamic (*e.g* cyclic voltammetry (CV) (section 2.4.1.1) and pulse (galvanostatic and potentiostatic)) techniques [16]. Any kind of technique must ensure a sufficiently positive potential so the monomer oxidation can occur. In the case of Py this potential is around 0.8V vs. Ag/AgCl in aqueous solution.

In general, the kind of electrical signal has an impact on the nucleation rate occurring in the first steps of the synthesis mechanism and, thus, in the way in which the chain growth proceeds, which at the same time influences its morphological structure, surface area and porosity.

In the pulse potentiostatic methods (Figure 4) cathodic ($E_c$) and anodic ($E_a$) rectangular pulses [17] are applied for $t_c$ and $t_a$ periods of time, respectively. The duration and the value of each pulse varies according to the experiment of interest and, thus, in the particular case of PPy the Ea has a longer duration

since the oxidation of the monomer is needed to induce the polymerization. With a pulse of this kind one would be, almost simultaneously, synthesizing and reducing the polymer and so, slower formation kinetics, which would favor a more ordered electrodeposition would be expected.

Additionally, during the reduction the formed polymer contracts due to the temporal leaving of the counter-ion, so the influence of this kind of signal on the final degree of doping is of special interest. However, this class of electrical signal has only been briefly studied on the synthesis of CPs, with the exception of the works of Mitchel *et al.*, who obtained highly ordered films using this method[18].

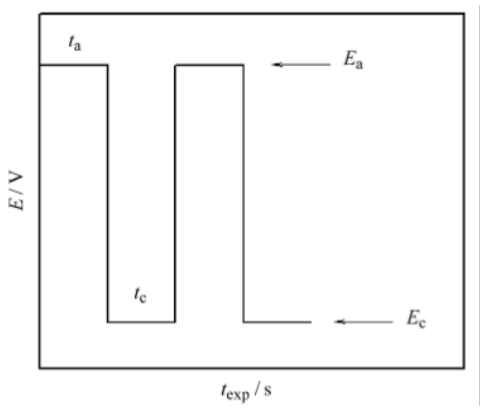


**Figure 4.** Schematic representation of the potential variation in a pulse potentiostatic method[19]

2.2.2. Chemical synthesis

Although electrochemical synthesis is preferred when preparing polymers for electrode coatings, thin layer sensors and microtechnology, chemical synthesis has the advantage of being easily scalable[11]. Using this method the polymer is obtained as a powder, the oxidation (or reduction) is done by a chemical agent and the synthesis variables are significantly reduced due to the fact that no electrochemical cell is needed. However, the polymerization mechanism is similar to that observed for the electrochemical methods[6].

Similar to electrochemical synthesis, the synthesis variables for the chemical method affect the nature of the process and the features of the final polymer. In particular, the chemical nature of the oxidant (its formal potential) and its concentration have an effect on the polymerization kinetics and charge delocalization[6]. The solvent and the pH of the media may favor the formation of short chain colloids. The use of strategically substituted monomers allows an ordered polymerization and the obtention of polymers with better electrical conductivities. In the same way, the substituents may improve the solubility of the polymeric powders[6]. Last, and in the same way as electrochemical synthesis, the relation [monomer]/[dopant] and the temperature is very important.

### 2.3. Doping and conductivity of CPs

CPs are intrinsically conducting and owe, in large proportion, their physicochemical properties to a process of *ionic insertion*, which they experiment during or after the synthesis. This process is known as *doping* and differs from solid state doping due to the fact that in the former there is no atom substitution but rather interstitial substitution (within the polymeric chains) of species.

This doping can be anionic or cationic and, based on this, it has been defined in the following manner: **1)** *p-doping,* which is associated to an oxidation that introduces negative charges to the polymer and **2)** *n-doping,* which is associated to a reduction that introduces positive charges to the polymer[20]. The effect of *p-doping,* which is the most common because it is intrinsic to the oxidation synthesis mechanism, is presented next although the reasoning is analogue for *n-doping*.

A radical cation is formed when an electron is removed and one could think, in the first instance, that it would delocalize along the whole structure. However, it has been shown that this only occurs partially in CPs[20] and, thus, the radical cation is known as a *polaron*. It must be stressed that different from a simple electronic excitation, a *hole* is not formed in the valence band (VB) after *p-doping* but rather intermediate orbitals are formed between the valence band and the conductivity band (CB) due to a geometrical restructuration that is experimented by the CP[20]. When *p-doping* proceeds, *bipolarons* (partially delocalized dications) are formed. In this way, at low doping levels there are *polarons* and as the process continues bipolarons and, finally, bands of these are formed (Figure 5).

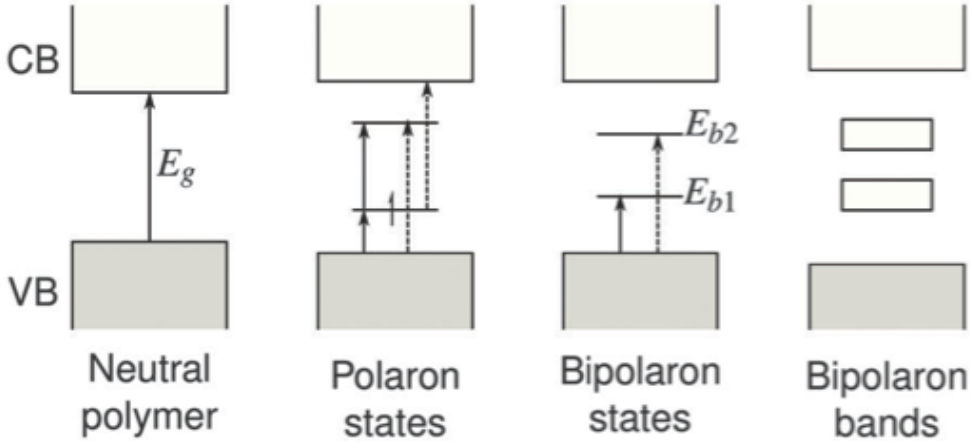


**Figure 5.** Schematic representation of the evolution of electronic bands in a CP after *p-doping* [21]

At relatively high doping levels (*e.g.* 35% for PPy), *bipolarons* are mobile after the application of an electric field and it is this phenomena the one that explains conductivity in CPs. Additionally, it must be noted that when doping levels close to 100% are achieved, as it has been the case with PTh, the *bipolaron* bands may combine with the VB and CB, producing metallic conduction[1]. On the other hand, PPy is characterized for being positively charged in its oxidized state while having neutral charge and being hydrophobic in its reduced state. This feature allows the incorporation of anions (dopants) during oxidative electropolymerization and the expulsion of them or insertion of cations ($C^+$), in case the incorporated anions ($A^-$) are too big, by means of a reduction (Figure 6) [22].

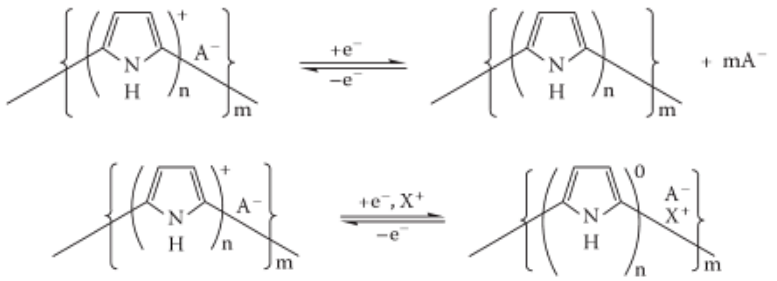

**Figure 6.** PPy doping [6]
Top: $A^-$ is small / Bottom : $A^-$ is big
$A^-$ is the anion (dopant)
$X^+$ is a cation

The chemical nature of the dopant has an important impact on the final properties of the polymer. In the first instance, it must be chemically and electrochemically stable under the synthesis conditions used because, otherwise, its decomposition products could interfere in the polymerization mechanism. Additionally, the dopant has an effect on the conductivity and the mechanical properties of the polymer. For example, aromatic anions with sulfonic groups induce a high crystallinity degree, which translate into better conductivities. On the other hand, the dopant also influences the ability of the polymer to interact with different solvents and structures[6].

## 2.4. Methods of investigation

### 2.4.1. Electrochemical methods

The main methods used in this study for the characterization of CP films are briefly discussed below.

#### 2.4.1.1. Cyclic voltammetry (CV)

In CV the potential is cycled, at a fixed rate, between two values (Figure 7) for a given number of cycles and the current response is measured[14] . A cyclic voltammogram (Figure 7) is obtained by plotting the current in the y-axis and the potential in the x-axis. The shape of the latter can be better understood by considering the electroactive species, as follows: As the potential reaches sufficiently negative values, the electroactive species is reduced and the *cathodic current* increases. Conversely, as the potential reaches sufficiently positive values, the electroactive species is oxidized and the *anodic current* increases. Both the *anodic* and the *cathodic currents* increase rapidly until the electroactive species is consumed at the electrode (redox reaction) and then decay as the solution surrounding the electrode is depleted of it[14]. The potential at which the cathodic and anodic currents reach maximum values are known as the cathodic ($E_{pc}$) and anodic ($E_{pa}$) potential, respectively.

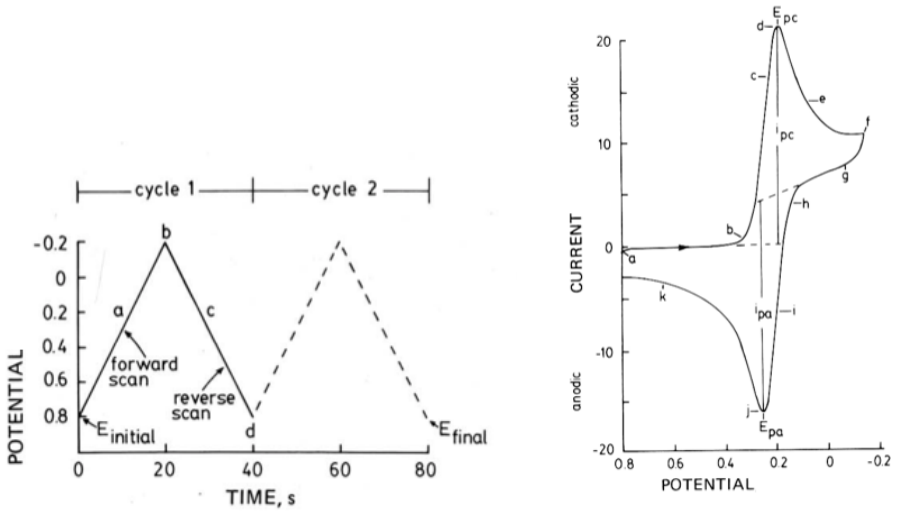


**Figure 7.** Voltages scan in CV (*left*) and cyclic voltammogram of a single electron reaction (*right*)[14]

2.4.1.2. Electrochemical impedance spectroscopy (EIS)

In the basic EIS experiment an alternating voltage, U(t), is applied to the system and the current response, I(t), is measured. Both signals can be represented as follows:

$$U(t) = U_m sin\,(\omega t) \qquad (1)$$

$$I(t) = I_m\, sin(\omega t + \vartheta) \qquad (2)$$

Where $\omega$ is the angular frequency of the sinusoidal potential perturbation, $\vartheta$ is the phase shift and $U_m$ and $I_m$ are the amplitudes of the sinusoidal voltage and current, respectively[11]. An expression analogous to Ohm's law allow us to calculate the impedance of the system, Z(t), which is a complex number composed of both a real (Z`) and an imaginary part (Z'').

$$Z(t) = \frac{U(t)}{I(t)} = Z' + iZ'' \quad (3)$$

The most basic system under study must have at least 2 electrodes and an electrolyte. It can be described by relating every process occurring in it with a circuit element (Figure 8), as follows[23]: **1)** the current in the bulk solution is transported mainly by ionic migration. This can be accounted by a solution resistance component ($R_{SOL}$). **2)** There is a transition between ionic and electronic conduction at the electrode/electrolyte interface and the charge transfer across it is accompanied by an electrochemical reaction at each electrode, known as *electrolysis.* This charge transfer is accounted by a so-called charge transfer resistance ($R_{CT}$). **3)** The electrolysis reactions can cause either an accumulation or depletion of species and charges around the electrode, which results in a concentration gradient that, consequently, causes diffusion from and to the bulk solution. This is expressed by a complex diffusion impedance element ($Z_{DIFF}$), which is sometimes referred to as a Warburg impedance ($Z_W$). **4)** Some species do not participate in *electrolysis* reactions at the applied potential but their charges are countered by opposite

charges in the electrode, thus forming a double layer capacitance ($C_{DL}$). This element is created from species different to those present in electrolysis and diffusion and, consequently, this element is in parallel with $R_{CT}$ and $Z_{DIFF}$.

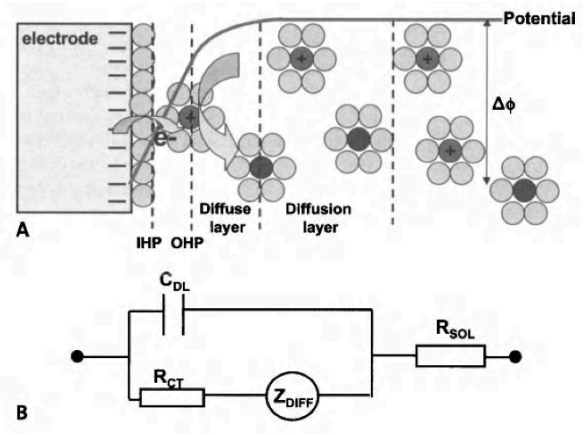


**Figure 8.** A) Basic interfacial electrochemical reaction with B) its associated (equivalent) circuit[23]
Inner Helmohltz plane (IHP) / Outer Helmholtz Plante (OHP)

In the present study EIS will be used as a tool for characterizing polymer (film) coated electrodes and the conditions will be such that no electrolysis reactions will occur. A general analysis of the main processes present in this system is shortly presented next: **1)** Electron transfer at the electrode/film interface. **2)** Transport of species (ions and solvent molecules) and electrons through the film**. 3)** Insertion of ions and solvent molecules at the film/solution interface and **4)** Transport of ions and solvent molecules in the solution[23]. This system is commonly described using the Randles Circuit, which is similar to that presented in Figure 8. The main difference lies in the fact that the parallel $R_{CT}$ –$C_{DL}$ combination now represents the electrode-film interface electron transfer and film-solution interface ion transfer[23].

Last, but not least, it must be pointed out that impedance data can be presented either as a Nyquist plot, a Bode (modulus) plot or a Bode (phase) plot (Figure 9).

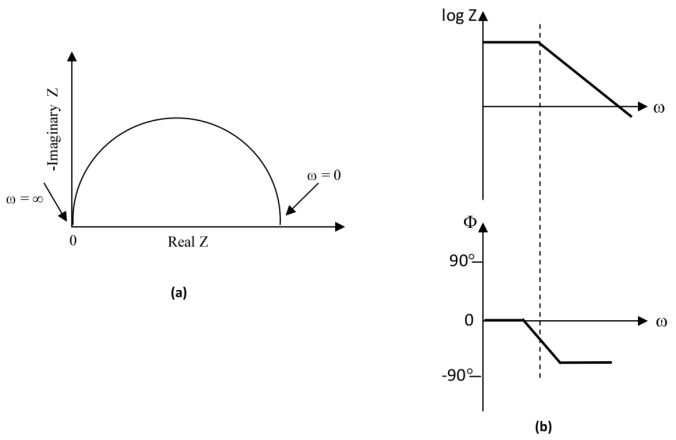


**Figure 9.** (a) Nyquist plot showing the real vs imaginary part of impedance. (b) Top: Bode (modulus) plot showing the variation of impedance (log Z) with frequency/ Bottom: Bode (phase) plot showing the variation of phase angle (Φ) with respect to frequency[24]

## 2.5. Properties and applications

The discovery that polymers with high electrical conductivity could be prepared widened the possibilities for the development of a great variety of applications; however, this is not the only useful property of CPs. Some of these properties and related applications, putting emphasis on PPy, are discussed below.

### 2.5.1. Electrodynamics – charge storage capacity

The ease with which PPy is oxidized and reduced can be translated in charge/discharge processes. This has been used in the development of rechargeable batteries which, when combined with a lithium cell and another electrode have reached cell potentials of, approximately, 3V. The energy densities reached with these batteries exceed, significantly, those obtained with nickel-cadmiun and lead-acid batteries.

### 2.5.2. Electrochromism

The dynamic properties of CPs also produce visual changes in them. Thus, PPy goes from being colorless to black after the application of positive potentials. In a similar way, PTh goes from red, in its oxidized state, to blue, in its reduced state[6]. This property finds an important application in smart windows and billboards.

### 2.5.3. Moldable chemical properties

The chemical properties of a CP may be modified according to the application in mind. In this way sensors based on a recognition process followed by a signal transduction process, which makes good use of the electrochemical properties of $CP_S$, may be developed. It has been shown that the recognition process can be achieved by the incorporation of enzymes, antigens and oligonucleotides, among other things, to the polymer. These can been incorporated to the CP by covalent bonding or as dopants[6].

# 3. EXPERIMENTAL

## 3.1. Reagents

Potassium ferricyanide ($K_3[Fe(CN)_6]$), 4-Amino-1-naphthalenesulfonic acid sodium salt hydrate, copper(II) chloride anhydrous, L-ascorbic acid (AA) and dopamine(DA) hydrochloride were supplied by Sigma Aldrich. Pyrrole(Py), Potassium chloride (KCl) and sodium hydroxide (NaOH) were supplied by Merck. Acetone was provided by the reagent store of the Chemistry Department at Universidad de los Andes. Alumina powder was supplied by EMS.

Pyrrole was purified by vacuum distillation and store under Nitrogen at -6ºC. All other reagents were used without any further purification. Solutions were prepared using ultrapure (type 1) water. Electrode cleaning was also done using ultrapure (type 1) water.

### 3.2. Equipment

All the synthesis and electrochemical characterizations were performed using a three-compartment cell in conjunction with a Metrohm Autolab PGSTAT302N with frequency response analyzer module (FRA32M) for impedance analysis operated with a computer interface using the NOVA software (version 1.10.5) for control and data handling. A glassy carbon electrode (GCE) (Area: 0.07 $cm^2$) from BASi was used as the working electrode (W); a platinum wire was used as the counter electrode (C) and a Ag/AgCl electrode from BASi was used as the reference electrode (R).

Raman spectra were recorded using the HORIBA XploRA ONE Raman microscope; Infrared (IR) spectra were recorded using a Nexus Thermo Nicolet 670 FT-IR; ultrapure (type 1) water was obtained from an EASYpure UV unit from Barnstead-Thermolyne Corporation and all the pictures were taken using a Motic SMZ-168 stereo microscopic with a 10 megapixel camera (Moticam 10) operated with Motic Images Plus 2.0 software.

### 3.3. Electrode cleaning

GCE cleaning before every synthesis was done following a standard protocol developed in our lab, which is described as follows: **1)** The electrode is polished in 1.0 µm alumina slurry by making figure-8 motions for 1 minute, then it is turned for 90 degrees and polished for 1 more minute. **2)** The alumina slurry is washed away from the GCE surface with abundant water and sonicated for 2 minutes in water (water 1). **3)** These steps are repeated using 0.3 µm alumina slurry. **4)** Step 1 is repeated using 0.05µm alumina slurry and then the GCE is sonicated for 5 minutes in fresh water (water 2). **5)** The GCE is anodized in a 0.1M NaOH solution at 1.8V during 10 seconds and then sonicated for 10 minutes in fresh water (Water 3). **6)** Finally the GCE is dried with nitrogen.

The Pt wire was cleaned with acetone and the Ag/AgCl electrode was rinsed with abundant water after every measurement and always stored in 3M KCl.

### 3.4. Synthesis

The conditions for every synthesis are specified hereunder. 10mL of solution were used in each case and every solution was purged with a nitrogen stream for 5 minutes and a nitrogen stream steady flux was maintained over the solution during the process. After every synthesis a 0.8V potential was applied for 15 s in fresh 0.1M KCl and the surface was thoroughly washed with abundant water.

#### 3.4.1. Preparation of $PPy/Cl^-$

##### 3.4.1.1. Pulse potentiostatic method

The conditions for the synthesis of $PPy/Cl^-$ performed by this method are specified in Table 1.

PPy/$Cl^-$

| Pulse potentiostatic method | | |
|---|---|---|
| Synthesis | Parameters | Solution |
| A | $E_a$ = 0.8V, $t_a$ = 10s<br>$E_c$ = -0.2V, $t_c$ = 2s<br>Nº Cycles = 60 | 0.2M Py and 0.1M KCl |
| B | $E_a$ = 0.9V, $t_a$ = 10s<br>$E_C$ = -0.2V, $t_c$ = 1s<br>Nº Cycles = 80 | 0.2M Py and 0.1M KCl |
| C | $E_a$ = 0.9V, $t_a$ = 10s<br>$E_c$ = -0.2V, $t_c$ = 1s<br>Nº Cycles = 66 | 0.2M Py and 0.1M KCl |

**Table 1.** Pulse potentiostatic method conditions used for the preparation of PPy/$Cl^-$
$E_a$ and $E_c$ correspond to oxidizing and reducing potential respectively. $t_a$ and $t_c$ are the times during which $E_a$ and $E_c$ are applied.

3.4.1.2. Galvanostatic method

A current of 10mA was applied through a 0.2M Py - 0.1M KCl solution for 5 minutes.

3.4.1.3. Potentiostatic method

A 0.8V potential was applied to a solution of 0.3M Py - 0.1M KCl for 150s.

3.4.2.Preparation of PPy/$ANS^-$

3.4.2.1. Pulse potentiostatic method

The conditions for the synthesis of PPy/$ANS^-$ performed by this method are specified in Table 2.

PPy/$ANS^-$

| Pulse potentiostatic method | | |
|---|---|---|
| Synthesis | Parameters | Solution |
| D | $E_a$ = 0.8V, $t_a$ = 10s<br>$E_c$ = -0.2V, $t_c$ = 2s<br>Nº Cycles = 130 | 0.2M Py, 0.15M $ANS^-$ and 0.1M KCl |
| E | $E_a$ = 0.9V, $t_a$ = 10s<br>$E_c$ = -0.2V, $t_c$ = 1s<br>Nº Cycles = 66 | 0.3M Py, 0.1M $ANS^-$ and 0.1M KCl |

**Table 2.** Pulse potentiostatic method conditions used for the preparation of PPy/$ANS^-$
$E_a$ and $E_c$ correspond to oxidizing and reducing potential respectively. $t_a$ and $t_c$ are the times during which $E_a$ and $E_c$ are applied.

3.4.2.2. Galvanostatic method

The conditions for the synthesis of PPy/$ANS^-$ performed by this method are specified in Table 3.

| PPy/$ANS^-$ | | |
|---|---|---|
| **Galvanostatic method** | | |
| Synthesis | Parameters | Solution |
| F | J = 10 $mA/cm^2$<br>t= 5min | 0.3M Py, 0.1M $ANS^-$ and 0.1M KCl |
| G | J= 3 $mA/cm^2$<br>t = 5min | 0.3M Py, 0.1M $ANS^-$ and 0.1M KCl |

**Table 3.** Galvanostatic method conditions used for the preparation of PPy/$ANS^-$
J is current density

3.4.2.3. Potentiostatic method

A 0.8V potential was applied to a solution of 0.3M Py, 0.1M $ANS^-$ and 0.1M KCl for 150s.

### 3.5. Cationic exchange

Applying a reductive potential (-0.4V) to the PPy/ANS- film in a 0.1M $CuCl_2$ solution did the insertion of Cu (II) ions. The potential was applied until the measured current was constant (approximately 30s).

### 3.6. Characterization

3.6.1.Electrochemical Methods

Every solution was purged with a nitrogen stream for 5 minutes and nitrogen stream steady flux was maintained over the solution during the process.

3.6.1.1. Cyclic voltammetry (CV)

The potential range, number of cycles and scan rate varied according to the sample and are specified in each voltammogram. Every CV started at 0V and finished at the respective end potential.

3.6.1.2. Electrochemical impedance spectroscopy (EIS)

The open circuit potential (OCP) was determined for each system using the OCP determination command in NOVA. The frequency response between 0.01Hz and 100kHz was obtained with a 10mV perturbation.

3.6.2.Other methods

3.6.2.1. Fourier transform infrared spectroscopy (FT-IR)

IR spectra of films removed from the GCE surface were measured as KBr pellets between 400 and 4000cm$^{-1}$.

3.6.2.2. Raman Spectroscopy

Raman spectra were directly measured from the electrode with a 785 nm combinational light scattering (CLS) laser and a 1200 gr/mm (grooves per milimiter) grating. A near infrared (NIR) 10x objective and a charge couple device (CCD) detector were used. All spectra were recorded at 100x magnification.

## 4. RESULTS AND DISCUSSION

### 4.1. Electroactivity of potassium ferricyanide ($K_3[Fe(CN)_6]$)

The CV for potassium ferricyanide on a polished unmodified GCE is shown in figure 10. The $E_{pa}$ and $E_{pc}$ values are 0.337 V and 0.120 V respectively. This system was used throughout this study as a test of the GCE surface activity and its cleaning.

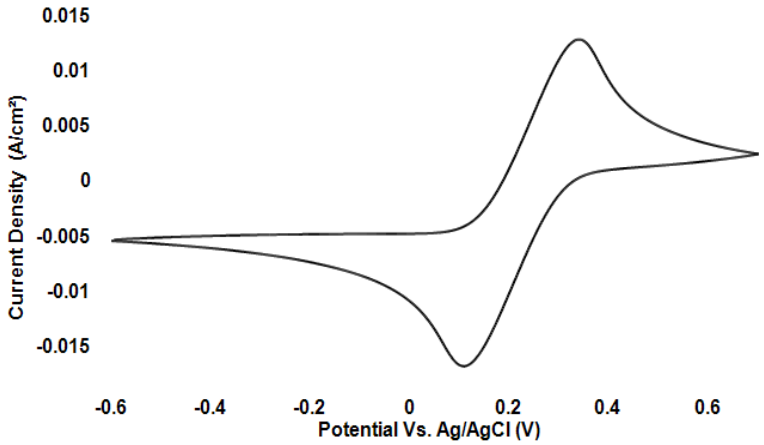


**Figure 10.** CV for the system $K_3[Fe(CN)_6]$) (0.2M) – KCl (0.1M) on a polished unmodified GCE
Scan rate: 100 mV/s
Nº Cycles: 6. Only the 3$^{rd}$ cycle is shown

The formal reduction potential ($E^0$) (4) for this system is 0.228V and the separation between peak potentials ($\Delta E$)(5) is 0.217 V, which highly differs from what is expected for a reversible reaction like this[14]. This may suggest that the surface is not completely available and, thus, the electron transfer is compromised. However, as there was no further improvement upon successive cleaning, this was chosen as the initial state of the surface.

$$E^{\circ} = \frac{E_{pa}+E_{pc}}{2} \qquad (4)$$

$$\Delta E = E_{pa} - E_{pc} \approx \frac{0.059V}{n} \qquad (5)$$

### 4.2. Electroactivity of sodium 4-amino-1-naphtalenesulfonate ($ANS^-$)

The CV for $ANS^-$ (Figure 11) shows a prominent anodic peak at 0.791V, a small cathodic peak at -0.608V and a redox couple at around 0.2V. The oxidation peak is in close agreement to what has been reported for 5-amino-2-naphthalenesulfonic acid[25] and it is attributed to the oxidation of the amine functional group to form a radical cation[26]. The fact that no corresponding cathodic peak is observed suggests that the formed radical undergoes a chemical reaction. This may be accounted by the ability of amines to bind to the surface of glassy carbon electrodes *via* the formation of the amine radical followed by a C-N bond formation [26]. This reaction can be similar to the electrografting based on diazonium salts, which has been widely studied for the modification of carbon surfaces with specific funcionalities. In this way, the amine radical would be stable at this potential and may thus react with the surface. This attachment reaction could be stimulated by the adsorption of the salt prior to its reduction. Moreover, this binding causes the current to diminish after each cycle indicating the progressive passivation of the GCE surface[27]. Figure 12 shows the proposed mechanism for this process occurring with 3-Aminobenzenesulfonic Acid[27], which has a similar structure to ANS.

The cathodic peak may be attributed to a reductive desulphonation [28] whereas the redox couple at around -0.2V may be assigned to the electroactivity of the naphthalene moiety in $ANS^-$[29]. However, further studies are needed to support these hypotheses.

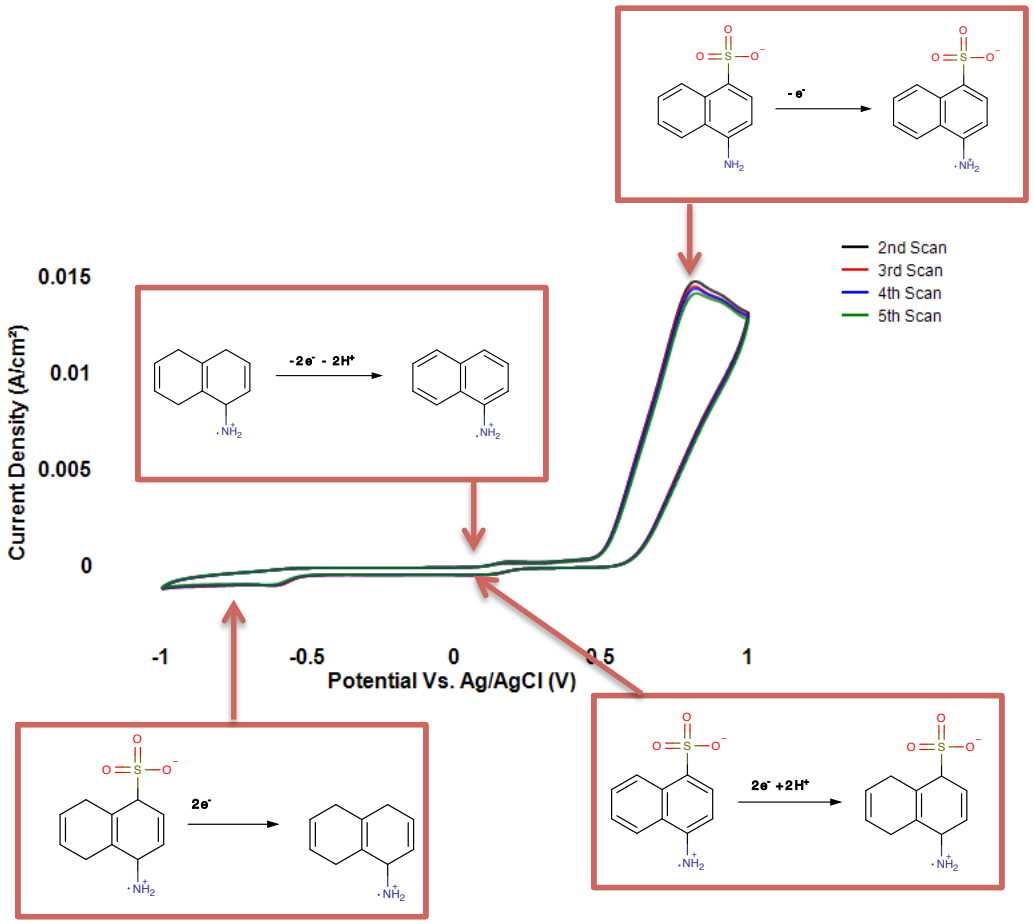


**Figure 11.** CV for the system $ANS^-$ (0.1M) – KCl (0.1M).
Scan rate = 100mV/s

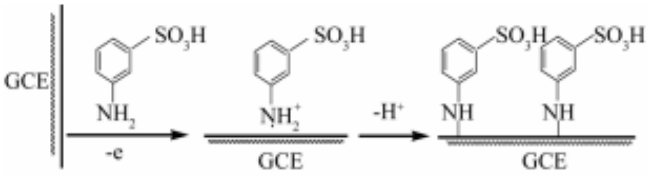


**Figure 12.** C-N bond formation between GCE and 3-Aminobenzenesulfonic Acid[27]

### 4.3. Electroactivity of Pyrrole

The first scan of the CV for pyrrole (Figure 13) shows an oxidation peak around 0.8V which corresponds to the formation of its radical cation[30]. The fact that no corresponding cathodic peak is observed suggests that the oxidized species immediately reacts to form oligomers, which is in agreement with the Diaz's mechanism[12]. The reduction peaks found at successive cycles are, thus, attributed to redox reactions of high molecular oligomers[31]. Moreover the anodic peak displacement after the first scan is explained by the changes of the highest occupied molecular orbital (HOMO) of the forming oligomers with respect to that of the monomer[31]: The forming oligomers have extended conjugation, so their HOMO is at higher energy and, consequently, the oxidation is easier to achieve(Figure 14). Last but not least, the current increase

with number of cycles is attributed to the formation of the polymer as this causes an increase in the effective electrode area[32].

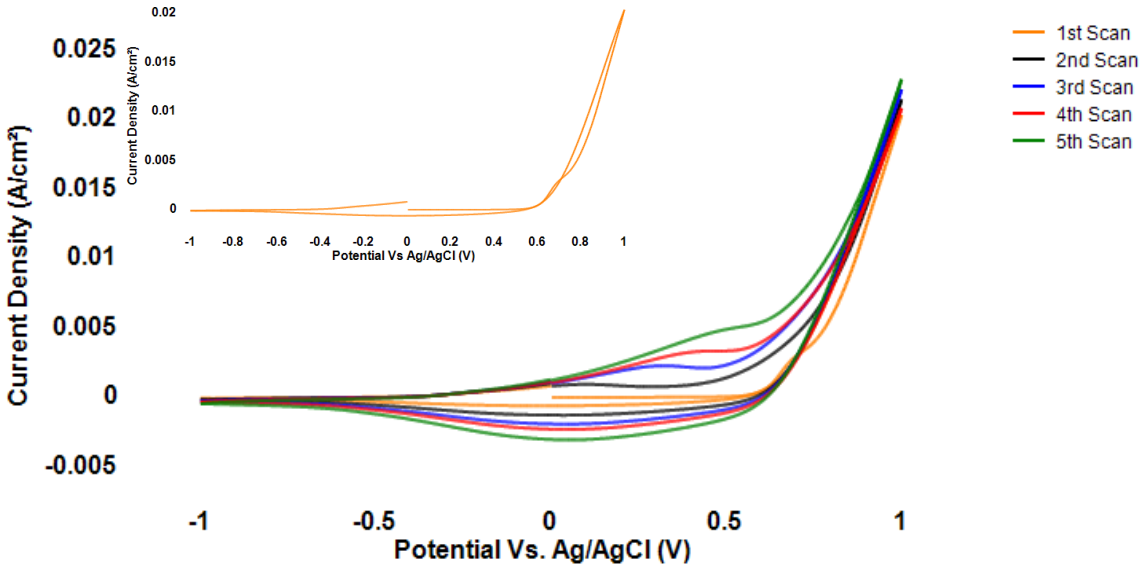


**Figure 13.** CV for the system Py (0.1M) – KCl (0.1M)
The inset shows the 1st scan, which corresponds to the monomer
Scan rate: 100mV/s

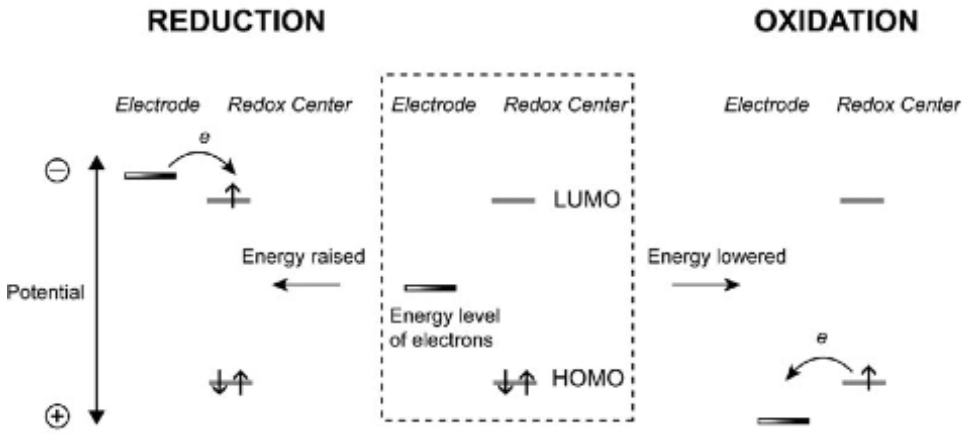


**Figure 14.** Normal picture of a redox process occurring on an electrode surface[33] .
Raising the HOMO is equivalent to lowering the Fermi level (Energy level of electrons): The oxidation is facilitated.

### 4.4. Synthesis of PPy/$Cl^-$

4.4.1. Pulse potentiostatic method

4.4.1.1. Synthesis A

The oxidation of PPy yields a charged polymer with incorporated anions, whereas its reduction is accompanied either by expulsion of anions or incorporation of cations (See *Theory*). The former is known to occur when the dopant is the chloride ion ($Cl^-$)[34] as is the case. The fact that two redox couples are observed in the CV for PPy/$Cl^-$ prepared by synthesis A (Figure 15) suggests that the synthesis method generates a polymer with different chain lengths, which causes the polymer to behave as a two-polymer system. This could be due to the oscillating nature of the electrical signal applied to the electrode, which could favor different nucleation rates. In addition, the fact that the anodic and cathodic peaks of each couple are not symmetric indicates that the film does not follow a Nernstian behavior and may be ascribed to some kinetic limitations of the redox reactions which must arise from the transport of ions in the film (Figure 16) [35]. This is supported by the observed displacement of all the peaks as the scan rate is increased, which indicates that the polymeric film obtained is of considerable thickness and thus presents a predominant diffusive behavior. The thickness of the coating ($d_n$) can be calculated (6) by using Faraday's law assuming: 1) a two electron mechanism, 2) the current efficiency is 100%, 3) a PPy density (ρ) of 1500 kg $m^{-3}$ and 4) a pyrrole molar mas (M) of 67 x$10^3$ kg $mol^{-1}$.

$$d_n = \frac{QM}{2F\rho} \qquad (6)$$

Where $Q$ is the area specific overall charge for electropolymerization and F is the Faraday Constant (96483.339 $Cmol^{-1}$). For this film, $Q$= 4.97 C $cm^{-2}$ and $dn$ = 1.10 µm.

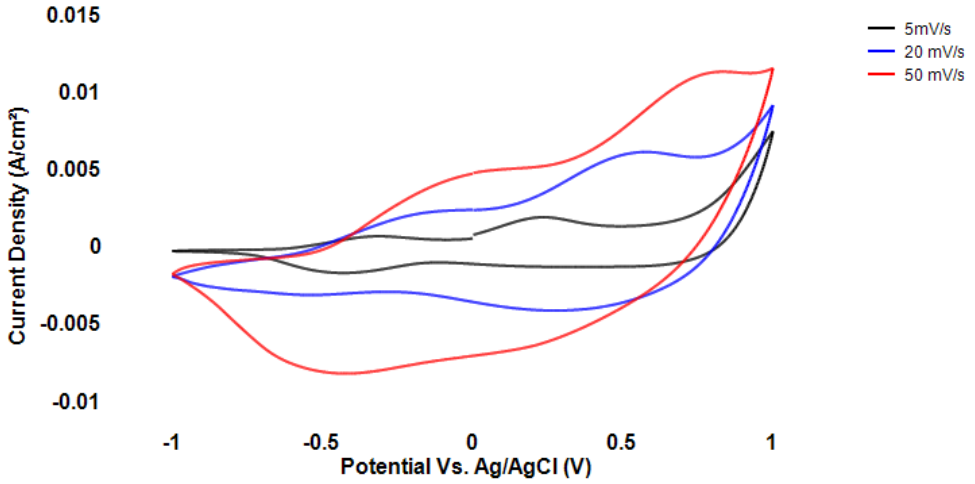


**Figure 15.** CV for PPy/$Cl^-$ (Synthesis A)
Nº Cycles = 6. Only the 3rd cycle is shown

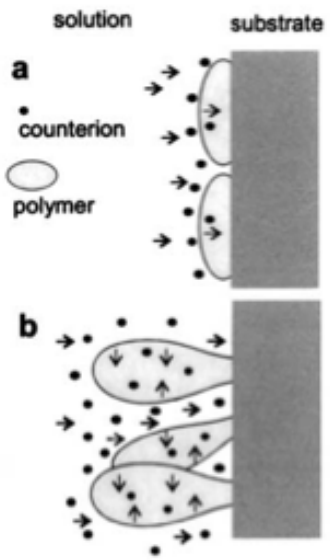


**Figure 16.** Schematic representation of the main transport process in a polymeric film. (a) Thin films and (b) thicker films showing complex porous structures. Arrows indicate ionic transport.[16]

The Nyquist plot obtained for this system is shown in figure 17. The shape of it suggests a mainly diffusion controlled process which is not totally accounted by the proposed circuit (Randles Circuit) as can be seen from the fit. However, the development and/or used of more complex equivalent circuits imposes a deeper analysis of the system and is out of the scope of this study. Therefore, the Randles circuit values will be used to compare the effect of the different synthesis methods on the final electric properties of the polymer.

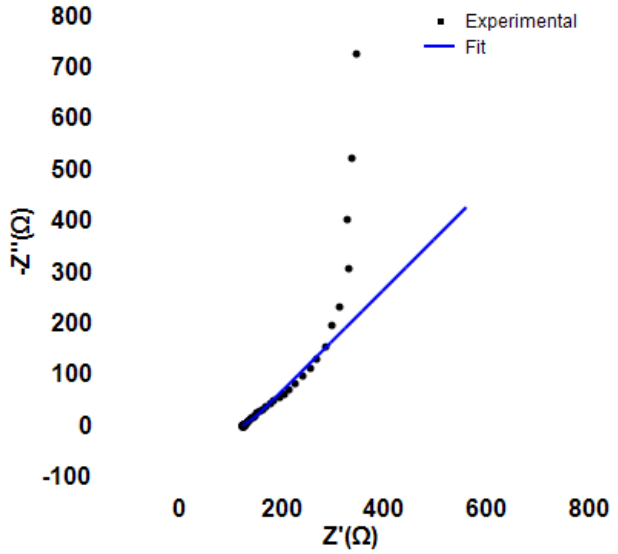


**Figure 17.** Nyquist plot for the system PPy /$Cl^-$ (Synthesis A)
$R_{SOL}$= 124Ω, $R_{CT}$=138.35 Ω$cm^{-2}$, $C_{DL}$= 2.02966 mF $cm^{-2}$, $Z_W$= 6.58 mMho

The pictures taken before and after the synthesis of PPy/$Cl^-$ by this method are shown in figure 18. It is clear that a complete, homogeneous coverage of the GCE surface was not obtained indicating that further improvement of the method was needed.

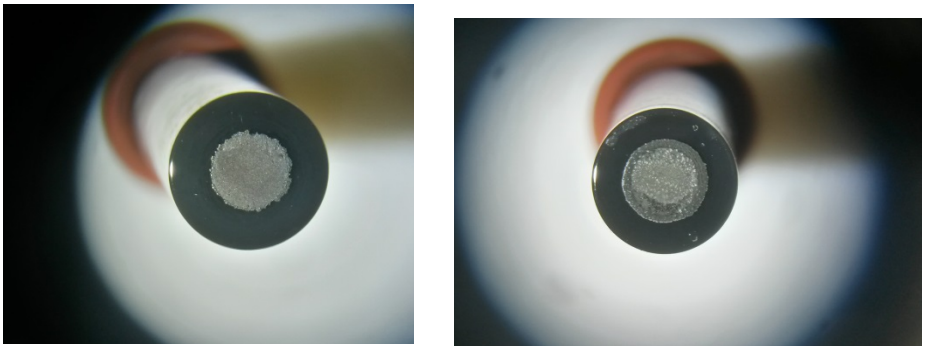

**Figure 18.** Picture of the GCE taken before (*Left*) and after (*Right*) synthesis A

4.4.1.2. Synthesis B

The CV for PPy/$Cl^-$ prepared by synthesis B (Figure 19) is very similar to that obtained for PPy/$Cl^-$ prepared by synthesis A (Figure 15), in the fact that a two-polymer system behavior can also be observed as is shown by the presence of two redox couples (especially when the scan rate is 50mV/s), however, two clear peaks are observed when the scan rate is 5mV/s, indicating ion exchange capabilities. Additionally, the peaks are not symmetric with scan rate, which also suggest a thick polymer. However, it must be stressed that in this case the current density increased significantly, which could be ascribed to better ion exchange capabilities of the polymer and/or film thickness. For this film, $Q$= 17.1 C $cm^{-2}$ and $dn$ = 3.94 µm which correlates with the observed shape of the CV.

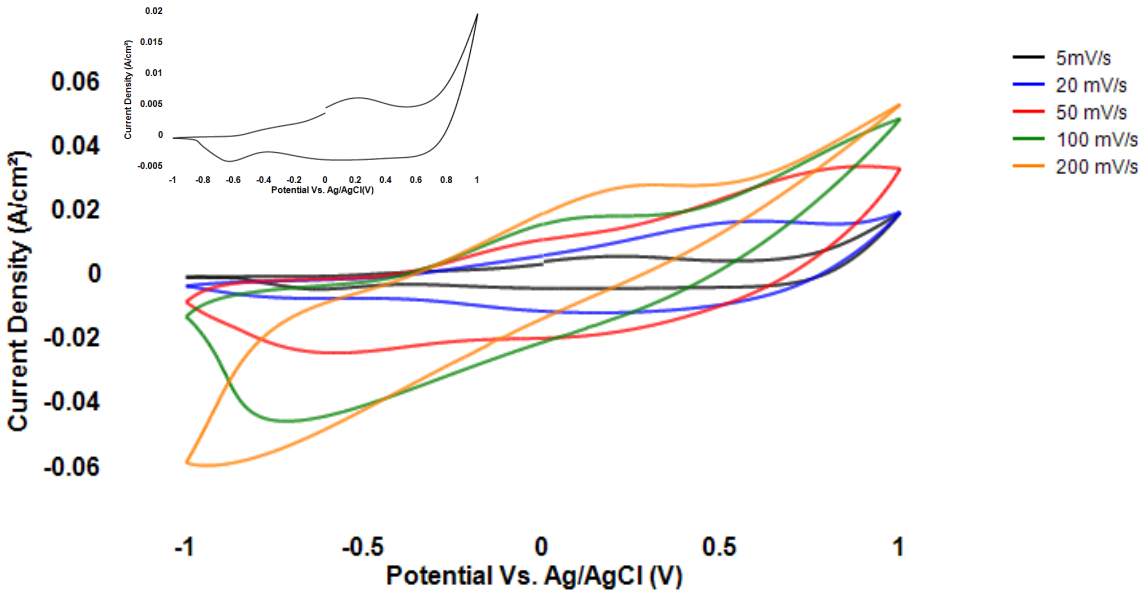


**Figure 19.** CV for PPy prepared by the pulse potentiostatic method (conditions B)
Nº of Cycles = 6. Only the 3rd cycle is shown. Inset shows 5mV/s

On the other hand, the pictures (Figure 20) of the GCE show a complete homogeneous surface coverage indicating an improvement with respect to synthesis A. However, the method still needed to be modified in order to avoid having thicker parts (in the outer parts of the surface).

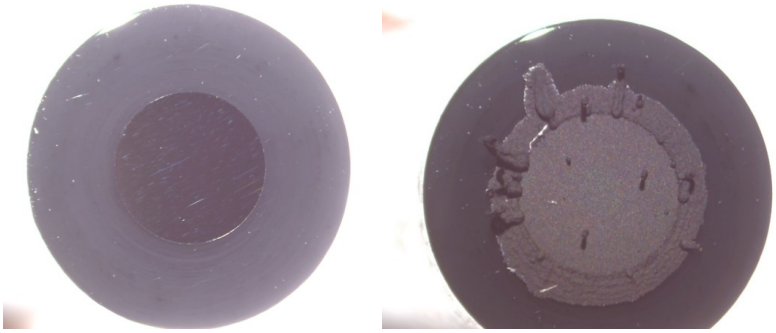

**Figure 20.** Picture of the GCE taken before (*Left.*) and after (*Right*) PPy synthesis B
A different GCE was used from this synthesis onwards, thus explaining the differences with Figure 18(*Left*).

4.4.1.3. Synthesis C

The picture of the GCE(Figure 21) taken after synthesis C suggests a better surface coverage in comparison with conditions A and B as the film covers most of the GCE surface and there are no significantly thicker areas. For this film, $Q$= 13.8 C $cm^{-2}$ and $dn$ = 3.5 μm. This indicates that a variation in the synthesis time translates in a variation of the film thickness.

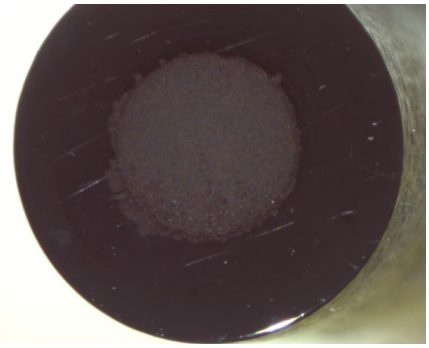

**Figure 21.** GCE surface after Synthesis C

On the other hand the Nyquist plot (Figure 22) for this film shows a mixed diffusion and charge-controlled process, which better correlates with the Randles Circuit. It is interesting to note that there was an increase in the $R_{CT}$ and a decrease in $C_{DL}$ values with respect to PPy prepared by synthesis A. The former may be explained by the increase in thickness; the latter could indicate that the presence of shallowly trapped ions (Figure 23) predominates in the film prepared by synthesis A: these can form an ionic double layer near the polymer chains, thus explaining the increase in capacitance[36].

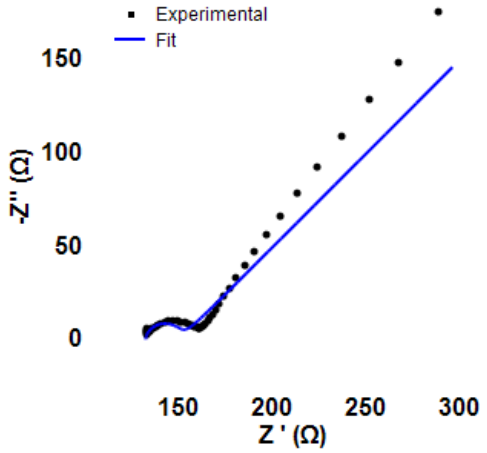


**Figure 22. .** Nyquist plot for PPy/$Cl^-$(synthesis C)
Solution: KCl (0.1M)
$R_{SOL}$= 134 Ω, $R_{CT}$= 253.23 Ωcm$^{-2}$, $C_{DL}$= 0.06364mF cm$^{-2}$, $Z_W$= 6.10 mMho

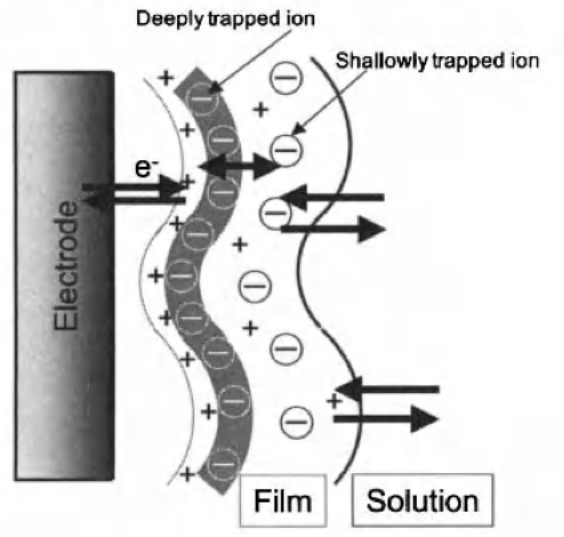


**Figure 23.** Schematic representation of the different ion trapping modes in a polymer film [23]

This polymer was also investigated using Raman spectroscopy (Figure 24). The Raman spectra of the bare GCE closely resembles that obtained by N.Tu, *et al*.[37], who report two bands at around 1590 and 1340 cm$^{-1}$ ,which correspond to crystalline graphite and less–organized graphitic forms, respectively. When comparing it to the spectra obtained after the modification it is clear that a surface modification was obtained. The most prominent bands correspond to C-N asymmetrical stretching (~ 1360 cm$^{-1}$), antisymmetrical C-H in-plane bending (~1229cm$^{-1}$), symmetrical C-H in plane bending (~ 1082 cm$^{-1}$) and ring deformation (~930cm$^{-1}$) associated with the presence of bipolarons[38], consequently indicating the formation of PPy.

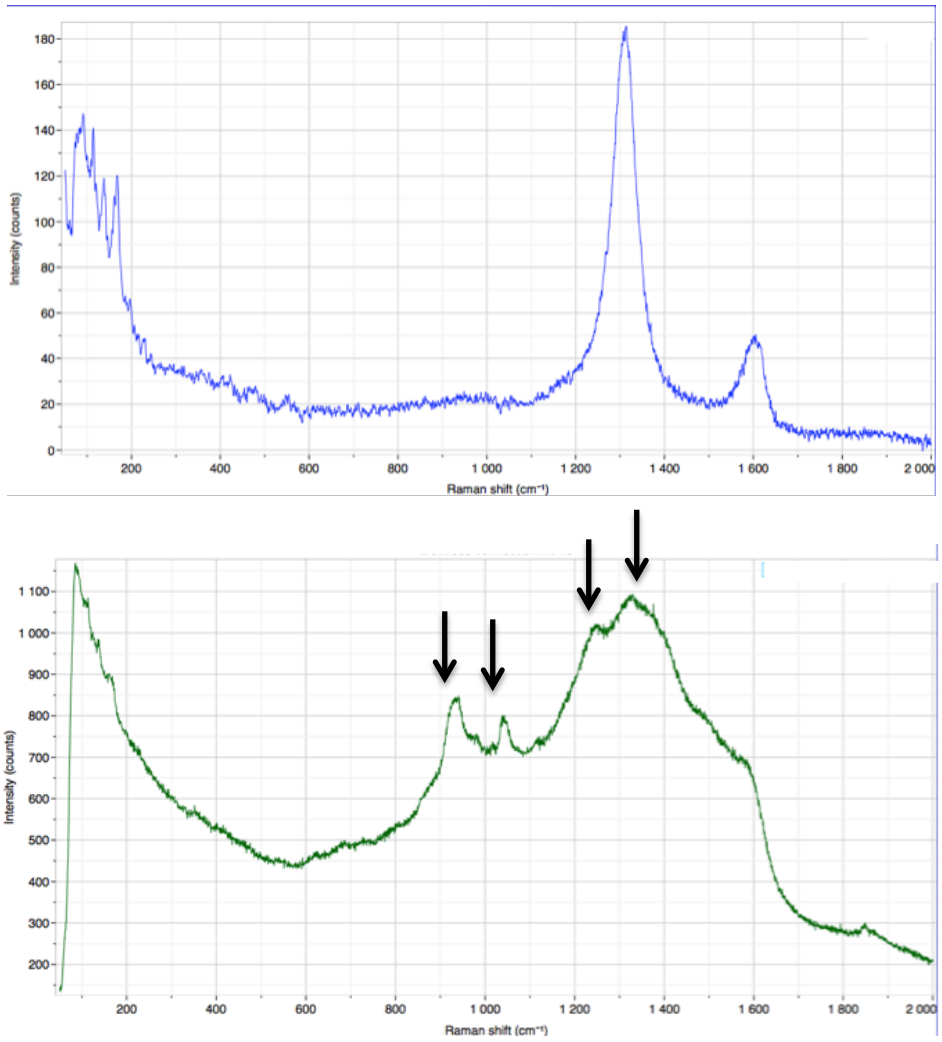


**Figure 24.**Raman spectra of bare GCE (*Top*) and PPy prepared by synthesis C (*Bottom*)

### 4.4.2. Galvanostatic method

The film obtained by this method showed a clear capacitive behavior rather than ion-exchange properties as can be seen in the absence of clear peaks in its CV (Figure 25). For this film, $Q$= 42.4 C cm$^{-2}$ and $dn$ = 9.8 µm. This indicates that film thickness does not necessarily translate into higher current density responses, as was initially thought, since this is the thickest film obtained so far and its current densities response are not the highest. This fact further supports the poor ion-exchange capabilities of this film.

The picture of this film (Figure 26) shows a rough, heterogeneous surface coverage. This supports the election of the pulse potentiostatic method as most convenient technique for developing hybrid materials of PPy with good ionic exchange properties.

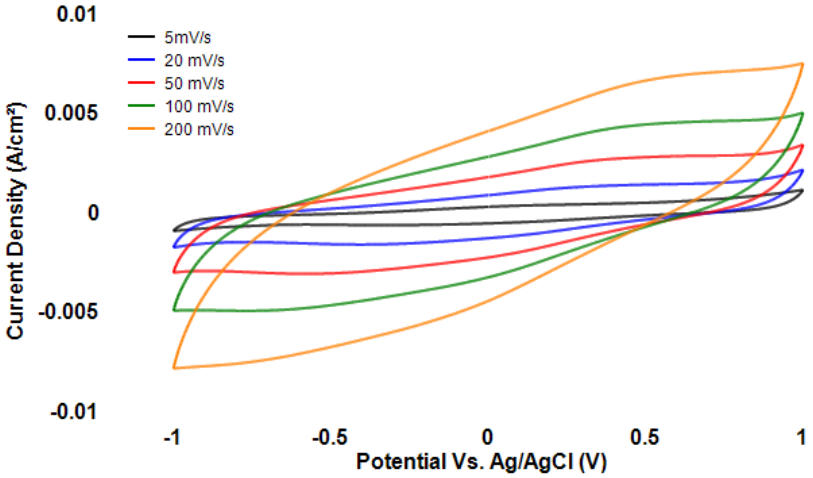


**Figure 25.** CV for PPy/$Cl^-$ prepared by galvanostatic conditions
Nº of cycles = 6. Only the 3rd cycle is shown

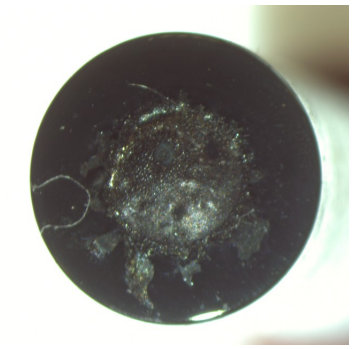

**Figure 26.**GCE surface after PPy/$Cl^-$ synthesis by galvanostatic method

### 4.4.3. Potentiostatic method

A synthesis by a potentiostatic method was also done as a mean for comparison. The picture of the GCE shows the surface is totally covered by a thin film. This can be ascribed to the fact that the potential was applied for only 150s, which is much less than what is needed to obtain complete surface coverage by a pulse potentiostatic method. For this film, $Q$= 1.30C $cm^{-2}$ and $dn$ = 0.030µm.

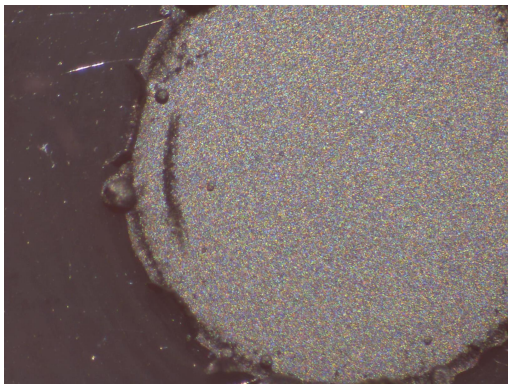

**Figure 27.** GCE surface after PPy/$Cl^-$ synthesis (Potentiostatic method)

## 4.5. Synthesis of PPy / $ANS^-$

### 4.5.1. Pulse potentiostatic method

#### 4.5.1.1. Synthesis D

As a preliminary test, the synthesis of PPy/$ANS^-$ was carried using optimal conditions (Synthesis C) for PPy/$Cl^-$, however, inspection of the GCE surface under the stereoscope showed no coverage. Consequently, a second synthesis was tried this time duplicating the number of cycles and leaving everything else unchanged. This method did not produce and observable surface coverage either. However, a CV for $[Fe(CN)_6]^{3-}$ (Figure 28) was done to verify the surface electroactivity and ,as can be seen, a very thin resistive film was deposited on the GCE surface. This may be attributed to the formation of an $ANS^-$ polymer, as has been shown to occur with 5-amino-2-naphthalenesulfonic acid[25](constitutional isomer of $ANS^-$)[25].

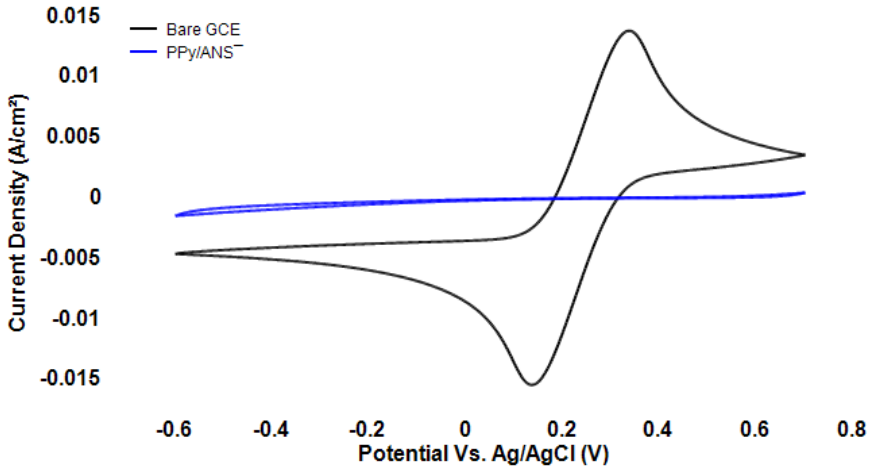


**Figure 28.** CV for the system $K_3[Fe(CN)_6]$) (0.2M) – KCl (0.1M)
GCE surface after synthesis D
Nº of cycles = 6. Only the 3rd cycle is shown

4.5.1.2. Synthesis E

After modifying synthesis D by increasing the Py concentration (up to 0.3 M), a complete surface coverage was obtained (Figure 29) which indicates that $ANS^-$ competes with Py in the formation of a film.

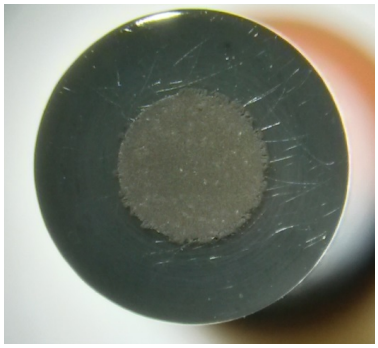

**Figure 29.** GCE surface after synthesis D

For this film, $Q$= 0.05429 C $cm^{-2}$ and $dn$ = 0.1366 µm. The low polymerization charge may be ascribed to the formation of an $ANS^-$ resistive film, which is further supported by a dramatic increase in the $R_{CT}$ (882.777 $\Omega cm^{-2}$) with respect to previously prepared PPy/$Cl^-$. This also agrees with the CV for $K_3[Fe(CN)_6]$) (Figure 28) obtained after synthesis D. This result and that from Synthesis D, evidence the high affinity of $ANS^-$ with the GCE surface that does not favor the electrodeposition of a hybrid material with PPy but the electrografting of $ANS^-$. This behavior can be changed in some extention if the pyrrole concentration is much higher than $ANS^-$ concentration, according to characterization results for Synthesis E.

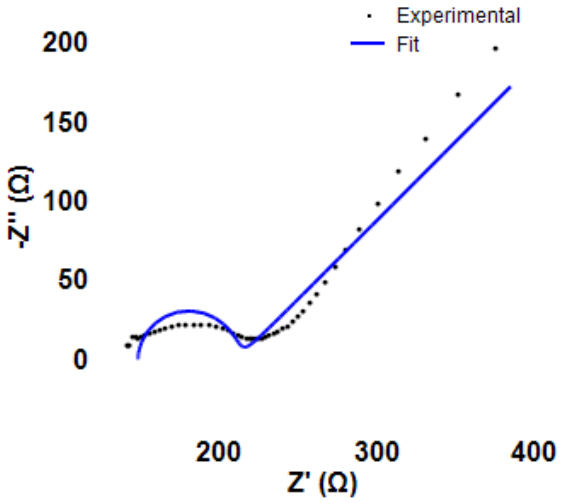


**Figure 30.** Nyquist plot for PPy/$ANS^-$ (synthesis E)
$R_{SOL}$= 148Ω, $R_{CT}$= 882.777 $\Omega cm^{-2}$, $C_{DL}$= 0.01711 mF $cm^{-2}$, $Z_W$= 5.14 mMho

The CV for this film (Figure 30) shows, especially when the scan rate is 5mV/s, clear ion-exchange capabilities. This resembles the results obtained for synthesis B.

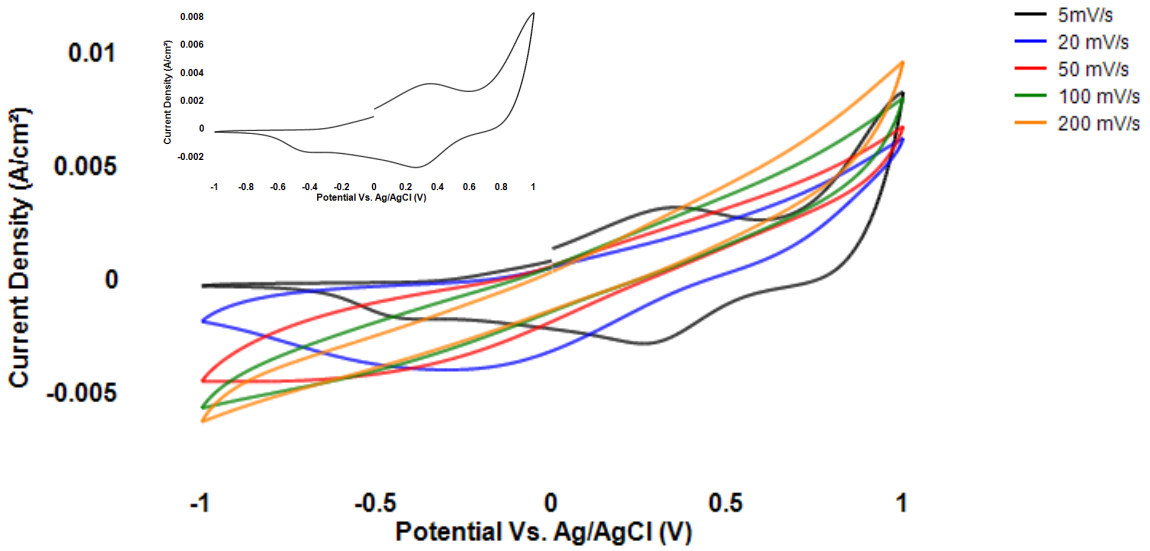


**Figure 31.** CV for PPy/ANS$^-$ (synthesis E)
Nº of cycles = 6. Only the 3$^{rd}$ cycle is shown.

Further characterization of this film was done by FT-IR spectroscopy (Figure 31). The band at 3420.82 cm$^{-1}$ corresponds to N-H stretch due to the Py units; the bands around ~2400cm$^{-1}$ corresponds to C-H stretch in aromatics which can be ascribed both to Py and ANS$^-$ units and the bands at 1573.42cm$^{-1}$ and 1408.25cm$^{-1}$ correspond to S=O stretch in sulfonates[39], which confirms the presence of ANS$^-$ in the film . The absence of a peak at around ~ 700 cm$^{-1}$ is proof of the PPy formation since this band is ascribed to C-H wag vibrations arising from adjacent 2,5 hydrogen atoms on the Py ring, which disappear during the oxidative electropolymerization[39].

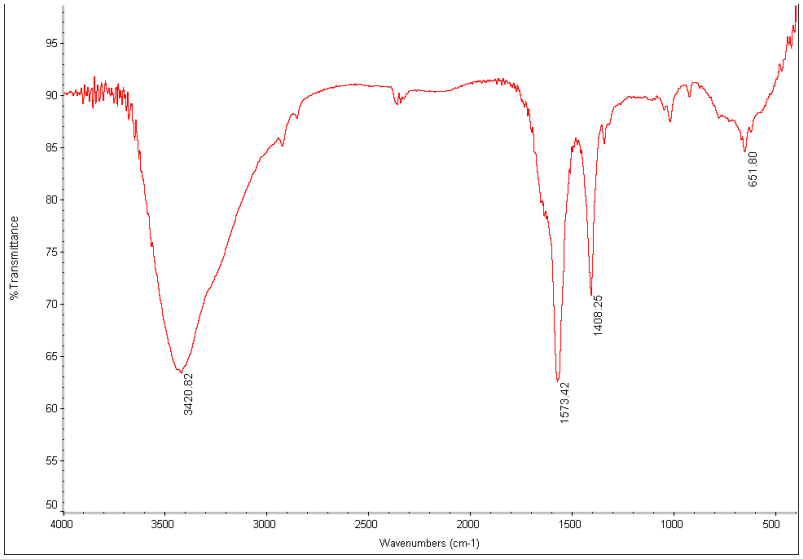


**Figure 32.** FT-IR of PPy/ANS$^-$ prepared by synthesis E

It must be noted that this film was not easily removed. It was still visible after polishing twice with each alumina and the CV for $[Fe(CN)_6]^{3-}$ (Figure 33) showed the surface was not cleaned. This indicated that the film binds covalently to the GCE surface *via* a C-N bond in a similar fashion to that presented in figure 12.

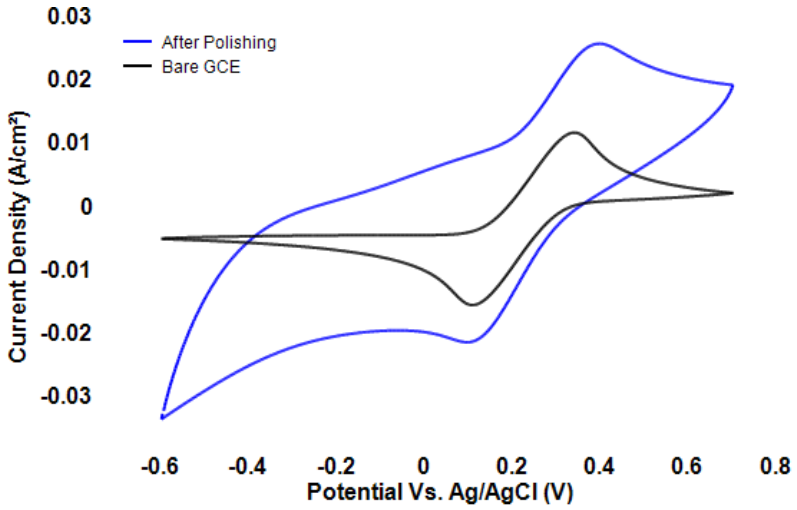


**Figure 33.** CV for the system $K_3[Fe(CN)_6]$ (0.2M) – KCl (0.1M)
GCE surface after polishing twice after synthesis E
Nº of cycles = 6. Only the 3rd cycle is shown

4.5.2. Galvanostatic method

As a mean for comparison, the preparation of $PPy/ANS^-$ was also carried using a galvanostatic method. However, a film could not be obtained under any of the current densities used since a white precipitated always formed (Figure 32). The latter was not characterized.

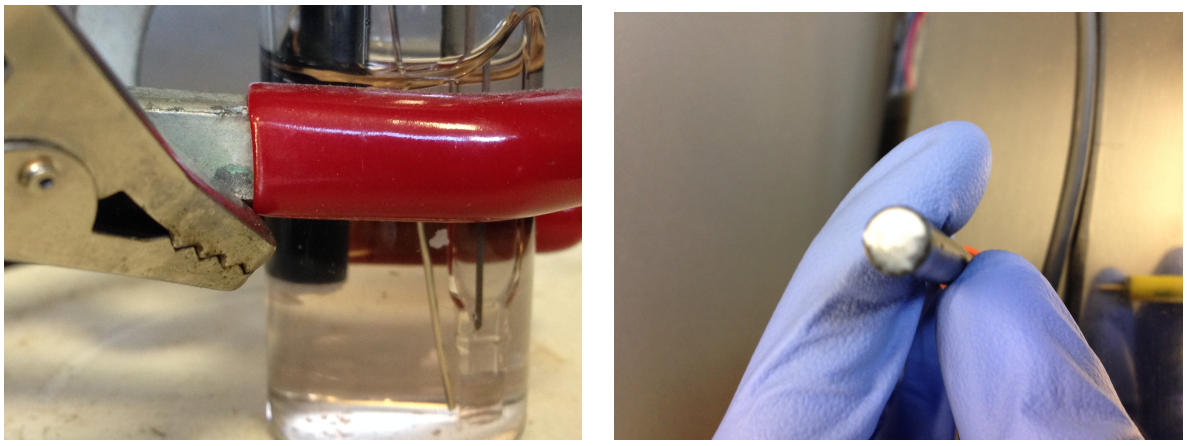

**Figure 34.** White precipitate obtained after $PPy/ANS^-$ synthesis by a galvanostatic method

4.5.3. Potentiostatic method

A potentiostatic method was also proposed for the synthesis of PPy/$ANS^-$ as a mean for comparison between different methods. As can be seen from the picture of the GCE surface after synthesis by this method (Figure 33), a white precipitate deposited on the surface of the electrode. However, it was lost after rinsing with water.

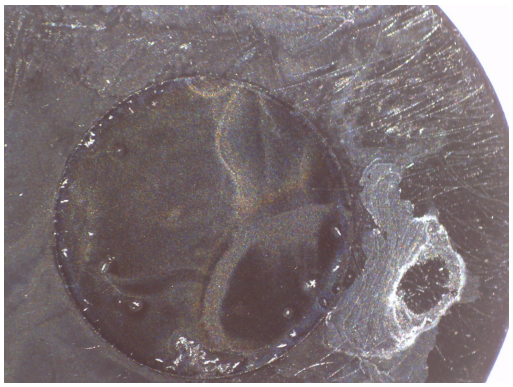

**Figure 35.** GCE surface after PPy/$ANS^-$ synthesis by a potentiostatic method

A CV for $K_3[Fe(CN)_6]$) (Figure 34) was done after rinsing the GCE surface with water to corroborate that nothing had deposited on it. The CV clearly resembles the one obtained after synthesis D (Figure 28), which further supports the idea that a resistive $ANS^-$ film was forming on the GCE surface.

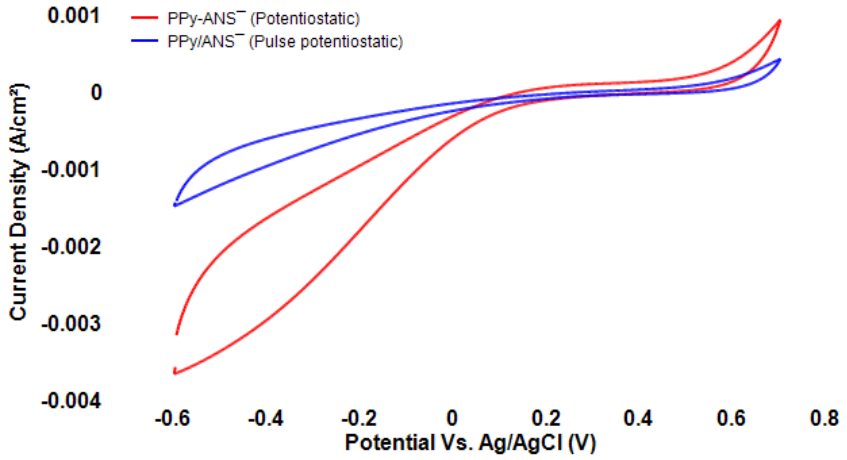


**Figure 36.** CV for $K_3[Fe(CN)_6]$)
GCE surface after preparation of PPy/$ANS^-$ potentiostatic and pulse potentiostatic method

This result clearly shows that $ANS^-$ clearly competes with Py since the same method produces total surface coverage when done without the presence of $ANS^-$ (See section 4.4.3).

At this point, it has been shown that the pulse potentiostatic method is the most convenient for obtaining a PPy/$ANS^-$ film on a GCE surface. This could be explained by the fact that during the oxidation pulses where PPy is formed, $ANS^-$ is incorporated in the interstitial spaces of the chain and, during the reduction pulses only ions close the surface can be eliminated since $ANS^-$ is big enough to remain in the interstitial spaces. Therefore allowing the PPy to be doped without favoring $ANS^-$ film formation as was supposed to occur with the other methods. However, this hypothesis needs further support and in-situ UV-visible spectroscopy and Energy-dispersive X-ray spectroscopy are proposed as a means for that.

### 4.6. Evaluation of PPy/$ANS^-$ as a Dopamine (DA) sensor

As a preliminary study to verify whether a PPy/$ANS^-$ coated GCE could be used as a DA *in vitro* sensor, the following preliminary test was conducted**:** A CV of a mixture of DA(100μM) and AA(500 μM) at pH = 7 (phosphate buffer,PBS) was done using a PPy/$ANS^-$ coated GCE (prepared by the same conditions as synthesis E) before and after Cu(II) ions insertion. This solution was chosen to simulate physiological conditions in which AA is present at much higher concentrations than DA[40]. Furthermore, it must be stressed that DA oxidizes at a potential close to AA.

First of all, it must be noted that the picture (Figure 35) of the GCE surface after the Cu(II) incorporation clearly shows that this process was successful, as can be seen from the color of the surface. This also supports the hypothesis that, when PPy is doped with voluminous anions, a reductive process results in the incorporation of cations, that is, a two-step doping process.

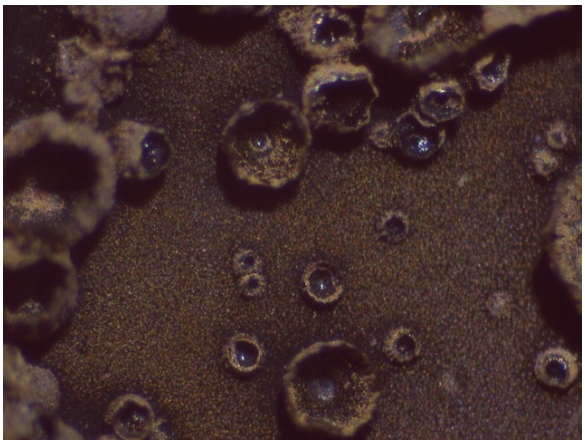

**Figure 37.** Picture of the PPy/$ANS^-$ coated GCE after Cu(II) insertion

On the other hand the CV of the mixture of AA and DA (Figure 36) indicates that neither the PPy/$ANS^-$ nor the PPy/$ANS^-$/Cu(II) allows the determination of DA, since no significant peaks can be detected. However, a significant decrease in the capacitive currents is obtained after Cu(II) insertion. This may be ascribed to the catalytic effect of Cu(II) towards catechol moieties[41]. This encourages the further use of Cu(II) in the development of this type of materials as possible DA sensors.

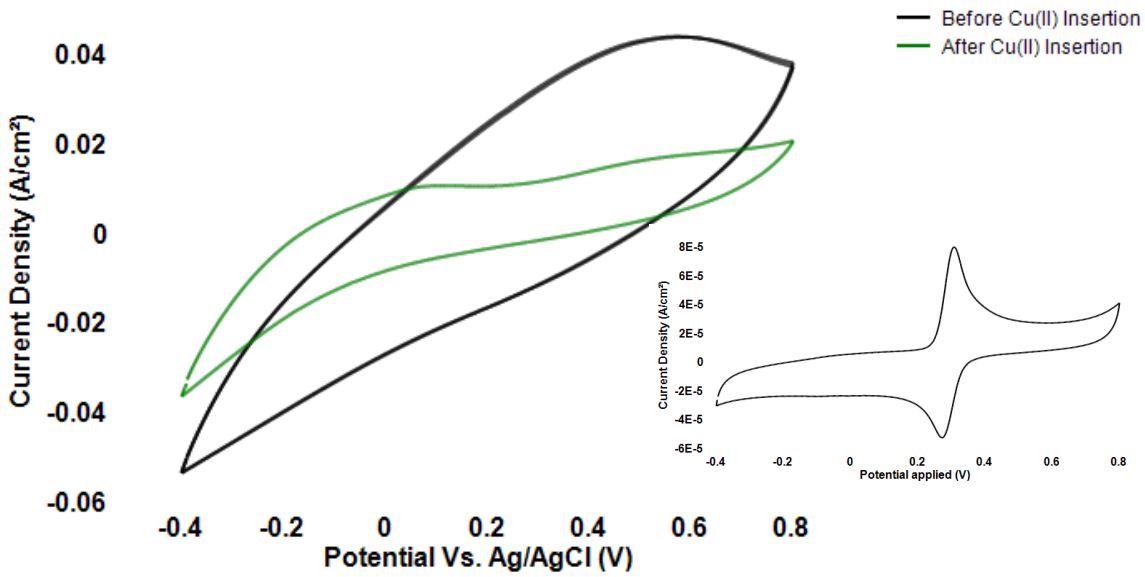


**Figure 38.** CV for a mixture of DA(100 µM )and AA(500 µM)
Scan rate = 100mV/s. Nº Cycles = 6. Only the 3rd is shown.
Inset shows a CV for DA(100 µM) using a bare GCE

## 5. CONCLUSIONS

It has been shown that a pulse potentiostatic method is the best technique for preparing a PPy/ANS$^-$ film on a GCE surface. This film shows good ionic exchange capabilities and binds covalently to the GCE surface, probably through the formation of C-N bonds between ANS$^-$ and the GCE surface. Neither potentiostatic nor galvanostatic methods work for this film as the former generates a resistive ANS$^-$ film and the latter produces an unknown precipitate. Additionally, it has been shown that ANS$^-$ competes with Py in the formation of a film and, thus, Py needs to be in much higher concentrations than ANS$^-$.

On the other hand, it was shown that Cu(II) ions may be incorporated to the PPy/ANS$^-$ films, thus confirming that cation incorporation can be achieved *via* two-step doping using voluminous anions. The PPy/ANS$^-$/Cu(II) showed better responses in the *in-vitro* determination of DA with respect to PPy/ANS$^-$ thus encouraging further studies on the development of DA sensors containing Cu(II) .

## 6. REFERENCES


(1) Chandrasekhar, P. *Conducting Polymers, Fundamentals and Applications: A Practical Approach*; Springer, 1999.
(2) Snook, G. A.; Kao, P.; Best, A. S. *J. Power Sources* **2011**, *196*, 1–12.
(3) Yim, J. H.; Joe, S.; Pang, C.; Lee, K. M.; Jeong, H.; Park, J.-Y.; Ahn, Y. H.; de Mello, J. C.; Lee, S. *ACS Nano* **2014**, *8*, 2857–2863.
(4) Tan, C. K.; Blackwood, D. J. *Corros. Sci.* **2003**, *45*, 545–557.
(5) Lange, U.; Roznyatovskaya, N. V.; Mirsky, V. M. *Anal. Chim. Acta* **2008**, *614*, 1–26.
(6) Wallace, G. G.; Teasdale, P. R.; Spinks, G. M.; Kane-Maguire, L. A. P. *Conductive Electroactive Polymers: Intelligent Polymer Systems, Third Edition*; 3 edition.; CRC Press: Boca Raton, 2008.
(7) Ramanavičius, A.; Ramanavičienė, A.; Malinauskas, A. *Electrochimica Acta* **2006**, *51*, 6025–6037.
(8) Nobel Media. The Nobel Prize in Chemistry 2000 - Advanced Information, 2000.
(9) Vernitskaya, T. V.; Efimov, O. N. *Russ. Chem. Rev.* **1997**, *66*, 443.
(10) Gamarra, J. D. Synthesis , optimization and characterization of a composite Heptafluorotanalate-polypyrrole (TaF72-/PPy) material with capacitive properties. Tesis de Maestría, Universidad de los Andes: Bogotá, Colombia, 2012.
(11) Inzelt, G. *Conducting Polymers A New Era in Electrochemistry*; Monographs in Electrochemistry; Springer Berlin Heidelberg, 2008.
(12) Sadki, S.; Schottland, P.; Brodie, N.; Sabouraud, G. *Chem. Soc. Rev.* **2000**, *29*, 283–293.
(13) Doyle, R. A Polypyrrole/Sulfonated Calixarene Modified Electrode for the Electochemical Detection of Dopamine. Thesis, 2011.
(14) Kissinger, P. T.; Heineman, W. R. *J. Chem. Educ.* **1983**, *60*, 702.
(15) Ma, W.; Ying, Y.-L.; Qin, L.-X.; Gu, Z.; Zhou, H.; Li, D.-W.; Sutherland, T. C.; Chen, H.-Y.; Long, Y.-T. *Nat. Protoc.* **2013**, *8*, 439–450.
(16) Zhang, J.; Kong, L.-B.; Li, H.; Luo, Y.-C.; Kang, L. *J. Mater. Sci.* **2010**, *45*, 1947–1954.
(17) Rajendran, V.; Gopalan, A.; Buvaneswari, R.; Vasudevan, T.; Wen, T.-C. *J. Appl. Polym. Sci.* **2003**, *88*, 389–397.
(18) Kiani, M. S.; Bhat, N. V.; Davis, F. J.; Mitchell, G. R. *Polymer* **1992**, *33*, 4113–4120.
(19) Zhou, H.; Wen, J.; Ning, X.; Fu, C.; Chen, J.; Kuang, Y. *Synth. Met.* **2007**, *157*, 98–103.
(20) Anslyn, E. V.; Dougherty, D. A. *Modern Physical Organic Chemistry*; University Science Books, 2006.
(21) Beverina, L.; Pagani, G. A.; Sassi, M. *Chem. Commun.* **2014**, *50*, 5413–5430.
(22) Durán Zambrano, M. H. Evaluación De La Influencia De Parámetros De Síntesis De Membranas De Polipirroles En El Proceso De Remoción De "pb+2" En Disolución Acuosa Mediante Eqcm (microbalanza Electroquímica De Cristal De Cuarzo). Tesis de Maestría, Universidad de los Andes: Bogotá, Colombia, 2011.
(23) Lvovich, V. F. *Impedance Spectroscopy: Applications to Electrochemical and Dielectric Phenomena*; Edición: 1.; John Wiley & Sons: Hoboken, N.J, 2012.
(24) *Modern Electrochemical Methods in Nano, Surface and Corrosion Science*; Aliofkhazraei, M., Ed.; InTech, 2014.
(25) Balamurugan, A.; Chen, S.-M. *Anal. Chim. Acta* **2007**, *596*, 92–98.
(26) Deinhammer, R. S.; Ho, M.; Anderegg, J. W.; Porter, M. D. *Langmuir* **1994**, *10*, 1306–1313.
(27) Zhang, L. *Am. J. Anal. Chem.* **2010**, *01*, 102–112.
(28) Grimshaw, J. *Electrochemical Reactions and Mechanisms in Organic Chemistry*; Elsevier, 2000.
(29) Hammerich, O.; Lund, H. *Organic Electrochemistry, Fourth Edition,*; CRC Press, 2000.
(30) Garfias-García, E.; Romero-Romo, M.; Ramírez-Silva, M. T.; Morales, J.; Palomar-Pardavé, M. *J. Electroanal. Chem.* **2008**, *613*, 67–79.
(31) Diaz, A. F.; Crowley, J.; Bargon, J.; Gardini, G. P.; Torrance, J. B. *J. Electroanal. Chem.*

*Interfacial Electrochem.* **1981**, *121*, 355–361.
(32) Skotheim, T. A.; Reynolds, J. *Conjugated Polymers: Theory, Synthesis, Properties, and Characterization*; CRC Press, 2006.
(33) Tran, E.; Duati, M.; Whitesides, G. M.; Rampi, M. A. *Faraday Discuss.* **2006**, *131*, 197–203.
(34) Khalkhali, R. A. *Russ. J. Electrochem.* **2005**, *41*, 950–955.
(35) Diaz, A. F.; Castillo, J. I.; Logan, J. A.; Lee, W.-Y. *J. Electroanal. Chem. Interfacial Electrochem.* **1981**, *129*, 115–132.
(36) Tanguy, J.; Mermilliod, N.; Hoclet, M. *J. Electrochem. Soc.* **1987**, *134*, 795–802.
(37) Nathan, M. I. *J. Appl. Phys.* **1974**, *45*, 2370.
(38) Jenden, C. M.; Davidson, R. G.; Turner, T. G. *Polymer* **1993**, *34*, 1649–1652.
(39) Scienza, L. C.; Thompson, G. E. *Polímeros* **2001**, *11*, 142–148.
(40) Goyal, R. N.; Gupta, V. K.; Bachheti, N.; Sharma, R. A. *Electroanalysis* **2008**, *20*, 757–764.
(41) Siegbahn, P. E. M. *JBIC J. Biol. Inorg. Chem.* **2004**, *9*, 577–590.